ECONOMIC GEOLOGY
RESEARCH INSTITUTE
HUGH ALLSOPP LABORATORY

**University of the Witwatersrand
Johannesburg**

MAGMATIC FRACTIONATION AND MIXING OF THE PGE-BEARING HONGGE LAYERED INTRUSION IN THE PANXI AREA. SW CHINA: CONSTRAINTS FROM TRACE ELEMENT AND Sr-Nd ISOTOPIC GEOCHEMISTRY

H. ZHONG, Y. YAO, S.F. HU, X.H. ZHOU, B.G. LIU, M. SUN, M.F. ZHOU, and M.J. VILJOEN

INFORMATION CIRCULAR No. 367

UNIVERSITY OF THE WITWATERSRAND

JOHANNESBURG

MAGMATIC FRACTIONATION AND MIXING OF THE PGE-BEARING HONGGE LAYERED INTRUSION IN THE PANXI AREA, SW CHINA: CONSTRAINTS FROM TRACE ELEMENT AND Sr-Nd ISOTOPIC GEOCHEMISTRY

by

H. ZHONG[1,3], Y. YAO[2], S. F. HU[3], X. H. ZHOU[3], B. G. LIU[3], M. SUN[4], M. F. ZHOU[4], AND M. J. VILJOEN[1]

([1] Department of Geology and CAMEG, School of Geosciences, University of the Witwatersrand, P/Bag 3, WITS 2050, Johannesburg, South Africa,
[2] Economic Geology Research Institute – Hugh Allsopp Laboratory, School of Geosciences, University of the Witwatersrand, P/Bag 3, WITS 2050, Johannesburg, South Africa,
[3] Institute of Geology and Geophysics, Chinese Academy of Sciences, Beijing 100029, China,
[4] Department of Earth Sciences, University of Hong Kong, Pokfulam Road, Hong Kong, China)

MAGMATIC FRACTIONATION AND MIXING OF THE PGE-BEARING HONGGE LAYERED INTRUSION IN THE PANXI AREA, SW CHINA: CONSTRAINTS FROM TRACE ELEMENT AND Sr-Nd ISOTOPIC GEOCHEMISTRY

ABSTRACT

The Fe-V-Ti-PGE-bearing Hongge layered intrusion in the Pan-Xi area of Sichuan Province, southwestern China consists, from the base upwards, of zones olivine clinopyroxenite (Cycle *I*), clinopyroxenite (Cycles *II, III*) and gabbro (Cycle *IV*). Abrupt reversals of major and trace element values at the boundaries of individual units suggest that new, more primitive magma was injected into the resident liquids in each cyclic unit. The new magmas originated from a mantle plume and were subjected to different degrees of contamination by continental lithospheric mantle and the upper crust. The homogeneous, decoupled Sr-Nd isotopes and cyclic variations of major and trace elements imply that each cyclic unit crystallized from a magma that was thoroughly mixed before crystallization. Assimilation of wall-rocks accounted for the PGE mineralization in Cycle *I*. Mixing between a primitive and an evolved magma resulted in the formation of the PGE-enriched layer in Cycle *II* and the magnetite layers in Cycles *II* and *III*.

_____oOo_____

MAGMATIC FRACTIONATION AND MIXING OF THE PGE-BEARING HONGGE LAYERED INTRUSION IN THE PANXI AREA, SW CHINA: CONSTRAINTS FROM TRACE ELEMENT AND Sr-Nd ISOTOPIC GEOCHEMISTRY

CONTENTS

—————————oOo—————————

MAGMATIC FRACTIONATION AND MIXING OF THE PGE-BEARING HONGGE LAYERED INTRUSION IN THE PANXI AREA, SW CHINA: CONSTRAINTS FROM TRACE ELEMENT AND Sr-Nd ISOTOPIC GEOCHEMISTRY

INTRODUCTION

Platinum group elements (PGE) are considered by the Chinese government to be of strategic importance as China is becoming one of the major consuming countries of platinum metal, in particularly the jewellery market. Recently, PGE geochemical anomalies in the Pan-Xi area of Sichuan Province, southwestern China have been recognized in layered igneous intrusions, such as the Panzhihua, Hongge, Xinjie, Baima and Taihe deposits (Fig.1, inset). These complexes have been hosts to numerous giant Fe-V-Ti deposits and Cu-Ni-sulphide mineralization, exploited since the early 1960s (Yao et al., 1993; Liang et al., 1998).

The Hongge intrusion is a typical example of a layered complex (Fig. 1), in which PGE mineralization has been reported from the lower part (PXGT, 1981). The PGE enrichment has recently been explained by a mixing model of magmas (Zhong et al., 2002), on the basis of the geochemical characteristics of the PGE and chalcophile elements (Cu, Ni). It has been suggested that each cyclic unit in the Hongge intrusion resulted from crystal fractionation and mixing between a primary and an evolved magma, and that the sulphide segregation played an important role in PGE differentiation (Zhong et al., 2002). However, the sources and characteristics of the parental magmas are still poorly understood. This paper presents new analytical data on trace elements in the vertical profile and Sr-Nd isotopic signatures of
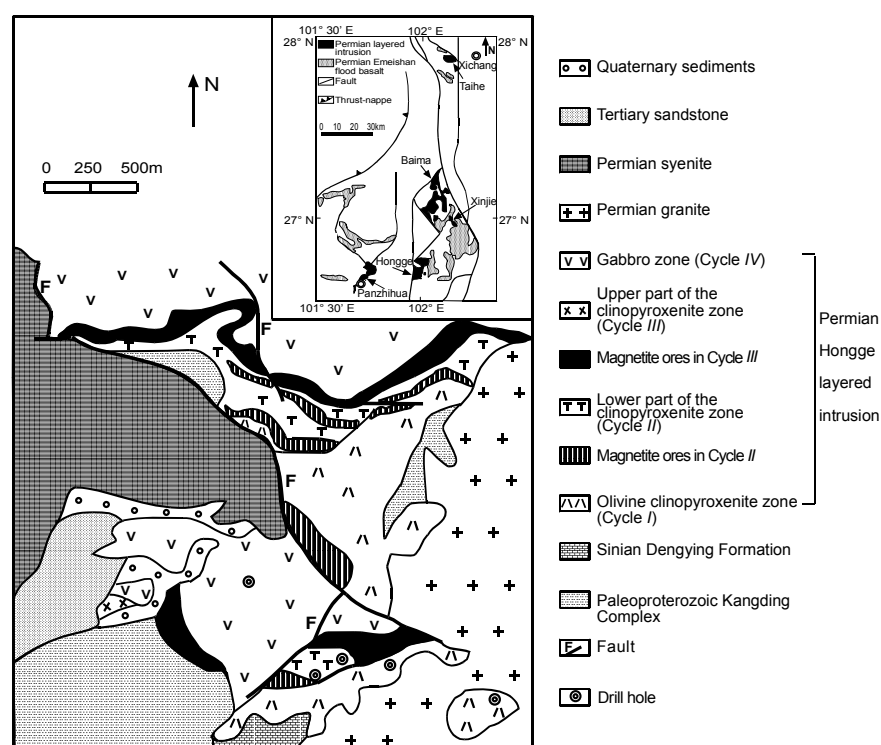

Figure 1: *Simplified geological map of the Hongge layered intrusion (modified after Yao et al., 1993). The division of cyclic units is illustrated in Figure 2. The upper right inset is the geological map of the Pan-Xi area of Sichuan Province, southwestern China, and shows the regional distribution of the layered intrusions (modified after Liu et al., 1985).*

cycle *I*. In combination with the published regional geology and geochemistry, the data are used to discuss the nature of parental magmas and to test the hypothesis of multiple injections of magmas for the Hongge intrusion.

GEOLOGICAL SETTING

The Pan-Xi area is located near the western margin of the Yangtze Craton, to the east of the Tibetan Plateau. The basement rocks of the Yangtze Craton, known as the Kangding Complex, comprise Precambrian granulite-amphibolite facies metamorphic rocks. The oldest recognizable strata form part of the Mesoproterozoic Huili Group or its equivalents, the Yanbian and Kunyang Groups, which are overlain by a thick sequence (> 9 km) of Sinian to Permian strata composed of clastic, carbonate, and metavolcanic rocks (SBGMR, 1991). Abundant Sinian granites and Neoproterozoic arc plutonic-metamorphic assemblages occur along the western and northern margin of the Yangtze Craton, suggesting the subduction of Rodinian oceanic lithosphere toward the Yangtze Craton during the period 760 to 860 Ma ages (Zhou et al., in press). The Craton was subjected to multiple-stage geotectonic movements, of which the late Variscan-Indosinian (280-230 Ma) rifting is the most significant (Cong, 1988). This event resulted in extensive emplacement of N-S trending, fault-controlled, ultramafic-mafic to felsic intrusions and the eruption of the Emeishan basalts which are 1500-2700 m thick and > 250000 km^2 in outcrop area (SBGMR, 1991).

The extensive Late Permian Emeishan Igneous Province is believed to have resulted from a mantle plume activity rather than a rifting environment (Chung and Jahn, 1995; Lu, 1996; Xu et al., 2001). The Emeishan basalts can be divided into high-Ti and low-Ti types, of which the low-Ti basalts are confined to the lower volcanic successions in the western part of the Province, whereas the high-Ti lavas predominate in the upper succession in nearly the entire region (Xu et al., 2001). Both the high and low-Ti magmas were subjected to contamination by upper crust and continental lithospheric mantle during ascent and emplacement (Xu et al., 2001).

The ultramafic-mafic intrusions described above are exposed along a 200 km-long belt, which is controlled by regional N-S-trending faults in the Pan-Xi area (Fig. 1, inset; Zhong et al., 2002). The layered intrusions in the central part of the Province are genetically related to the high-Ti basalts (Xu et al., 2001) and are ultramafic-mafic and mafic in composition. The mafic-type of intrusion consists of layered gabbro, with minor olivine-bearing gabbro, troctolite and anorthosite, although small amounts of ultramafic rocks occur in the lower portion of the igneous bodies (e.g., Panzhihua, Baima and Taihe). By contrast, the ultramafic-mafic complexes (e.g., Hongge, Xinjie) consist mainly of clinopyroxene-bearing peridotite, olivine-bearing clinopyroxenite, clinopyroxenite and gabbro. The most important PGE mineralization occurs in the ultramafic-mafic complexes, such as the Hongge intrusion (Liang et al., 1998; Zhong et al., 2002) and the Xinjie intrusion (Luo, 1981; PXGT, 1981; Zhang et al., 1998; Liang et al., 1998).

HONGGE LAYERED INTRUSION

The Hongge layered intrusion outcrops in an area of about 60 km^2 and intrudes dolomitic limestones of the Sinian Dengying Formation and granitic gneisses of the Kangding Complex.
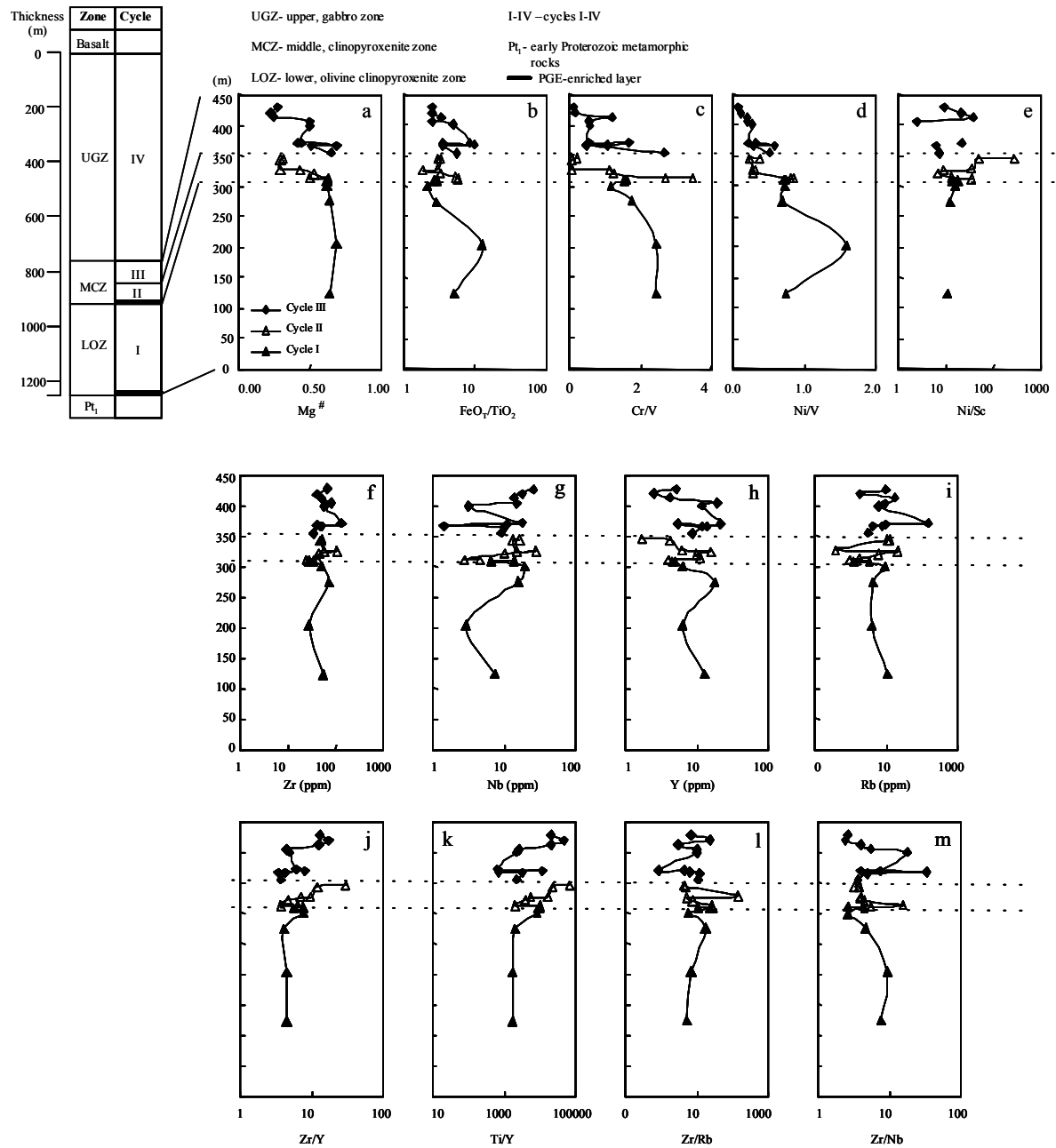
Figure 2: *Stratigraphy (modified after PXGT, 1987) and vertical variations of Zr, Nb, Y, Rb contents and values for Mg#, FeO$_T$/TiO$_2$, Cr/V, Ni/V, Ni/Sc, Zr/Y, Ti/Y, Zr/Rb and Zr/Nb within the three basal cyclic units of the Hongge intrusion. The locations of the samples are from Zhong et al. (2002). The values for Mg#, FeO$_T$/TiO$_2$, Cr/V, Ni/V, Ni/Sc were calculated from data published by Zhong et al. (2002).*

The Dengying Formation has been metamorphosed to marble in places adjacent to the intrusion (Zhang et al., 1999). The Emeishan basalts are present to the northeast of the Hongge intrusion and together with the later body were intruded by Permian granites and syenites (Fig.1). Zhong et al. (2002) described the petrology showing that igneous layering is well developed in the Hongge intrusion and consists of three zones. These include a lower olivine-clinopyroxenite zone (LOZ), a middle clinopyroxenite zone (MCZ), and an upper gabbro zone (UGZ). The LOZ and UGZ are characterized by single compositional cyclic units, but the MCZ is dominated by two compositional cyclic units (Fig. 2). The MCZ and

3

UGZ contain thick layers hosting disseminated V- and Ti-rich magnetite (Yao et al., 1993; Zhong et al., 2002). These authors considered that the cyclic units resulted from the periodic crystallization and fractionation of magmas. PGE-enriched layers occur in the lower parts of the LOZ and in the MCZ and are accompanied by Cu-and Ni-rich sulphide minerals such as pyrrhotite, pentlandite, pyrite, chalcopyrite and cubanite (Fig. 2, Liang et al., 1998; Zhong et al., 2002).

ANALYTICAL METHODS AND RESULTS

Samples for this study were collected from five drill holes in an area where abundant magnetite is present. Trace elements of the samples marked with an asterisk (*) were analyzed using a VG PlasmaQuad II ICP-MS at the Institute of Geology and Geophysics,

Table 1: Trace element concentrations (in ppm) and ratios for rocks from the Hongge intrusion

Sample no.	Cycle	Rb	Nb	Sr	Zr	Y	P	Sc	Ba	Ta	Hf	Cr/V	Ti/Y(*10³)	Zr/Y
MCZ1	III (top)	9.7	26	107	67	5.2	1475	17	-	-	-	0.10	20.9	12.9
MCZ2*	III	1.8	18	65	42	2.5	1396	11	74	2.12	1.6	0.13	24.6	16.6
MCZ3	III	17	13	79	53	4.1	1372	13	-	-	-	1.20	21.2	12.7
MCZ4*	III	8.5	15	104	84	19	1477	55	30	0.86	2.5	0.56	3.66	3.8
MCZ5*	III	5.7	3.2	105	57	12	1681	-	12	0.24	2.3	0.59	2.21	4.9
MCZ6*	III	151	18	387	130	21	1557	-	1530	0.91	2.2	0.56	0.62	6.1
MCZ7	III	9.6	11	78	43	5.4	1509	25	-	-	-	1.70	11.2	8.0
MCZ8*	III	7.4	1.4	471	46	14	1550	-	67	0.11	1.4	1.05	0.70	3.3
MCZ9	III	4.0	10	117	49	12	1399	51	-	-	-	0.49	3.06	4.2
MCZ10	III	2.9	9	90	33	8.7	1410	41	-	-	-	2.69	2.28	3.8
MCZ11	II	12	16	62	51	1.7	1409	3.2	-	-	-	0.24	63.8	30.2
MCZ12	II	11	13	75	49	4.1	1381	12	-	-	-	0.06	22.0	11.8
MCZ13*	II	0.39	15	50	58	6.0	1564	17	9.0	1.04	1.3	0.08	14.1	9.6
MCZ14	II	20	28	76	107	16	1447	37	-	-	-	1.15	5.28	6.8
MCZ15	II	5.7	10	112	45	10	1400	47	-	-	-	1.26	3.94	4.6
MCZ16*	II	1.69	2.8	89	43	11	1499	39	9.5	0.21	1.5	2.70	2.61	4.7
MCZ17*	II	0.9	4.5	47	25	4.0	1594	23	8.7	0.27	0.89	3.48	7.45	7.9
LOZ1	I	3.2	14	86	35	4.5	1475	38	-	-	-	1.61	9.84	7.8
LOZ2*	I	1.21	6.3	79.8	28	5.0	1389	32	3.0	0.68	1.2	1.54	6.23	6.4
LOZ3	I	8.5	20	102	50	6.5	1959	34	-	-	-	1.17	8.39	7.7
LOZ4	I	4.1	16	132	74	18	1890	40	-	-	-	1.75	2.07	4.1
LOZ5*	I	3.9	2.9	68.5	28	6.4	1431	-	19	0.34	0.70	2.45	1.67	4.3
LOZ6*	I (bottom)	10.6	7.3	233	56	13	1667	42	50	0.48	2.1	2.45	1.54	4.3

"-" not determined; "*" samples analyzed at the Institute of Geology and Geophysics, Chinese Academy of Sciences; the remaining samples were analyzed at the Department of Earth Sciences, Hong Kong University; Cr, V, Ti contents are from Zhong et al. (2002).
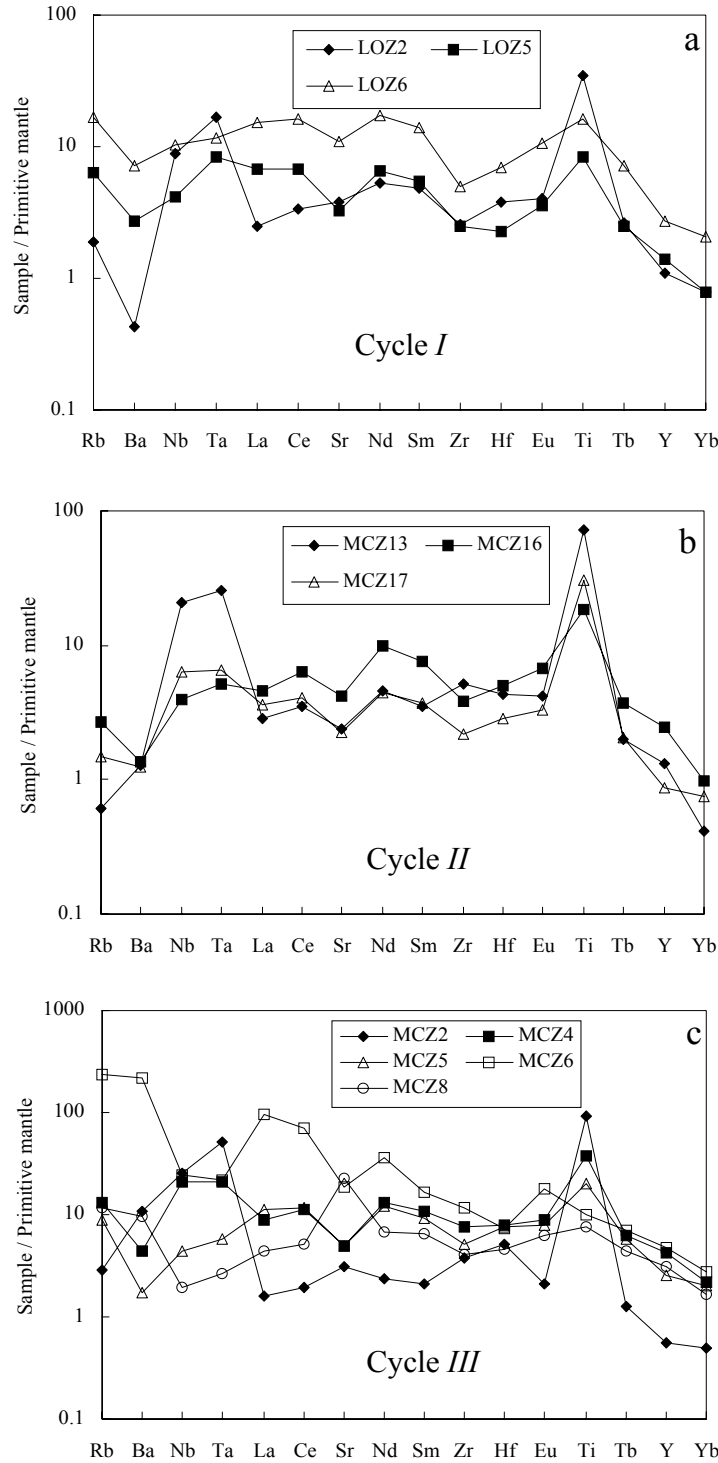
Figure 3: *Primitive mantle-normalized trace element concentrations in the Hongge intrusion. Normalizing values are from Sun and McDonough (1989).*

Chinese Academy of Sciences, Beijing (CAS). The trace elements from the remaining samples were determined on pressed powder pellets using a Phillips PW 2400 X-ray fluorescence spectrometer at the University of Hong Kong. The analytical precision for major oxides is better than 5 wt.%. The Sr-Nd isotope analyses were carried out using a VG-354 multi-collector instrument at the Institute of Geology and Geophysics (CAS), and the experimental details are described by Yang and Zhou (2001) and Hu (2001). Sr isotopic data was normalized to $^{86}Sr/^{88}Sr = 0.1194$; runs of NBS-607 Sr standards yielded a $^{87}Sr/^{86}Sr$ ratio

of 1.199965±12 (2σ) during the period of this study. Nd isotopic data was normalized to $^{146}Nd/^{144}Nd = 0.7219$; the mean of the measured $^{143}Nd/^{144}Nd$ ratio of the La Jolla Nd standard was 0.511863±7 (2σ). Total procedural blanks were less than 0.2 ng for Sr and 0.05 ng for Nd. The initial isotopic ratios were all corrected to 260 Ma (SHRIMP U-Pb zircon, pers. commun. with Zhou, 2002).

Table 2: Sr-Nd isotopic data for rocks from the Hongge intrusion

Sample No.	Rb (ppm)	Sr (ppm)	$^{87}Rb/^{86}Sr$	$^{87}Sr/^{86}Sr$	$(^{87}Sr/^{86}Sr)_I$	Sm (ppm)	Nd (ppm)	$^{147}Sm/^{144}Nd$	$^{143}Nd/^{144}Nd$	$\varepsilon_{Nd}(i)$
MCZ4	8.49	104	0.2366	0.707228 ±12	0.706353	4.16	14.9	0.1688	0.512538±16	-1.03
MCZ13	0.39	50.1	0.0227	0.705894 ±14	0.705810	1.49	5.35	0.1688	0.512612±27	0.42
MCZ16	1.69	89.0	0.0548	0.706061 ±15	0.705858	2.65	9.05	0.1773	0.512657±8	1.02
LOZ2	1.21	79.8	0.0440	0.706219 ±16	0.706056	1.91	6.65	0.1737	0.512622±9	0.45
LOZ5	3.99	68.5	0.1681	0.706625 ±15	0.706003	1.93	7.67	0.1520	0.512568±13	0.12
LOZ6	10.6	233	0.1315	0.706489 ±12	0.706003	6.07	24.7	0.1487	0.512419±8	-2.68

Various elemental concentrations and ratios are plotted against stratigraphic height within the LOZ and MCZ (Fig. 2). As shown in Figure 2a-e, the curves show a classic saw tooth pattern

with abrupt reversals at the beginning of each cycle. In addition, values for $Mg^#$ [$Mg^#$ =$Mg^{2+}/(Mg^{2+}+Fe^{2+})$], FeO_T/TiO_2, Cr/V, Ni/V decrease upwards within each cyclic unit, whereas Ni/Sc are quite variable. Across individual units Nb contents increase while Y contents decrease upwards; Zr and P contents are relatively constant while Rb contents are considerably variable (Table 1; Fig. 2f-i). At the transition zone of individual new units Nb and Rb contents clearly decrease whereas Y contents remarkably increase (Table 1, Fig. 2g-i). In addition, Zr/Nb decreases while Zr/Y and Ti/Y increase upwards within each cyclic unit, whereas Zr/Rb is variable (Table 1, Fig. 2j-m). One sample, contaminated by a syenite dyke (MCZ6), is marked by extremely high Rb, Sr, Zr, Y and Ba contents.

In the primitive mantle-normalized spidergrams, one sample (LOZ6) from the base of the Cycle *I* displays a significantly negative Sr anomaly and a markedly positive Ti anomaly. The other two samples (LOZ2, 5) from the Cycle *I* are characterized by significant enrichment of Nb and Ta relative to Ba, and slight Sr depletion and marked Ti enrichment (Fig. 3a). An obviously positive Nb and Ta anomaly compared to Ba, a slightly negative Sr anomaly and a significantly positive Ti anomaly, are shown in the samples from the Cycle *II* (Fig. 3b). Trace element distribution patterns are highly variable for the samples from the Cycle *III* (Fig. 3c). One sample (MCZ8) from the base of this cycle exhibits marked enrichment of Rb and Ba relative to Nb and Ta, a strongly positive Sr anomaly and a slight enrichment of Ti. By contrast, one sample (MCZ2) from the top of this cycle displays significantly positive Nb, Ta and Ti anomalies and slight enrichment of Sr. Two other samples (MCZ4, 5) show clear enrichment of Nb and Ta relative to Ba, and marked Sr depletion and Ti enrichment. However, the sample (MCZ6) contaminated by the syenite dyke is characterized by strongly positive Rb and Ba anomalies compared to Nb and Ta, as well as significant Sr depletion and a markedly positive Eu anomaly.

As shown in Table 2, the initial Sr isotopic compositions show a restricted range of slightly enriched source(s) in the three basal cycles of the Hongge intrusion, whereas the initial Nd isotopic compositions exhibit a relatively wide range of slightly enriched to depleted source(s).

DISCUSSION

In layered intrusive complexes, the trace element data, especially the incompatible trace elements, provide information on compositions of the trapped liquid, whereas the whole-rock major element chemistry reflects the cumulus mineralogy (Cawthorn and McCarthy, 1985; Wilson et al., 1999). Zhong et al. (2002) argued that the cyclic units of the Hongge layered intrusion may have resulted from crystal fractionation and mixing between a primitive and evolved magma on the basis of the geochemical characteristics of PGE and chalcophile elements. The incompatible trace-element and Sr-Nd isotopic study in the present paper can therefore provide more detailed geochemical constraints on the source(s) and mixing model of magmas.

Source(s) of parental magmas and magma evolution

The values for $Mg^#$, FeO_T/TiO_2, Cr/V and Ni/V consistently decrease upwards within the three cyclic units and show an abrupt increase between the transition zones of the units. The former is consistent with fractional crystallization of magmas. The vertical increase of Nb contents and values for Zr/Y, Ti/Y and Zr/Nb show incompatible behavior, which can also be related to the fractional crystallization of the magmas. The almost constant P contents may be attributed to the occurrence of a small amount of intercumulus apatite in the three cycles. The

highly variable Rb contents may be due to surface alteration in some of the samples. The observation that Zr contents are relatively constant while Y contents decrease upwards in each cyclic unit seems to be inconsistent with the normal fractional crystallization trends for mineral compositions. However, the Zr and Y may not be perfectly incompatible (Cruft, 1966; Walker, 1969; Cawthorn and McCarthy, 1985). Zr is present in magnetite analyzed by Walker (1969) and does not behave as a perfectly incompatible element in the Upper Zone of the Bushveld Complex (Cawthorn and McCarthy, 1985). Although there is no marked correlation between Zr and FeO_T (Fig. 4a), a good positive correlation between Zr and TiO_2 (Fig. 4b) indicates that the titaniferous magnetite may concentrate Zr as it is a common cumulus mineral throughout the entire Hongge intrusion. As a result, a strong decoupling of Zr and P has taken place on a sample to sample basis (Fig. 4c). The poor correlation of S with Zr (Fig. 4d) shows that crystallization of the sulphide is not obviously controlled by the trapped liquid, which is different from that of the Bushveld Complex (Wilson et al., 1999). Similarly, Y shows compatible behavior in the Hongge intrusion because apatite is a mineral that concentrates Y, as suggested by Cruft (1966) and Walker (1969), which is consistent with the positive correlation of Y with P (Fig. 4e). But the proposal that apatite also concentrates Nb (Cruft, 1966; Walker, 1969) is not supported by the poor relationship between Nb and P (Fig. 4f) in the present study.

Simple fractional crystallization cannot explain the abrupt increase of $Mg^{\#}$, FeO_T/TiO_2, Cr/V and Ni/V across the boundary of individual units and the geochemical trends of Nb contents, and values for Zr/Y, Ti/Y and Zr/Nb, shown in the profile (Fig. 2). The saw tooth pattern of the trace elements and their ratios throughout the intrusion is possibly related to a mixing model as suggested by Zhong et al. (2002). The incompatible trace element ratios avoid the uncertainty of random variations in the proportion of trapped liquids (Cawthorn, 1983). The abrupt change of the values for Zr/Y, Zr/Nb and Ti/Y across the transition zone of individual cycles therefore supports the addition of a new magma to the remaining liquid. It appears that the new magma has different ratios of trace elements from the evolved magma.
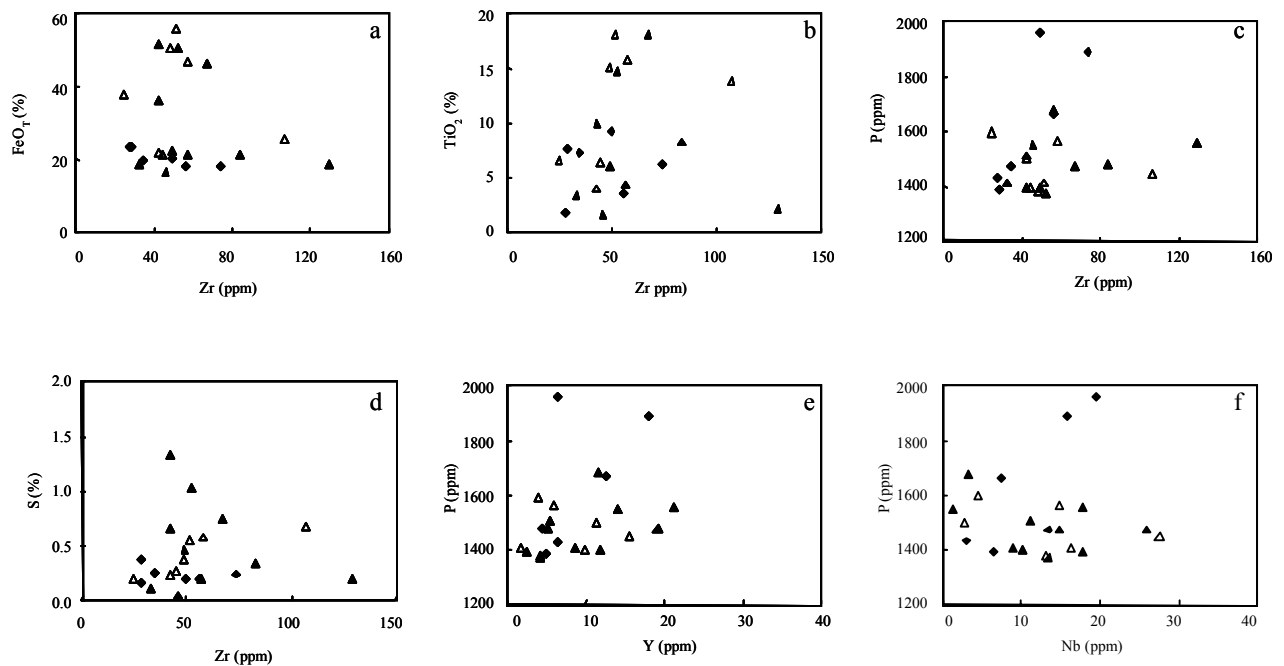

Figure 4: *Variations of FeO_T, TiO_2, P and S vs. Zr, and Y, Nb vs. P for the Hongge intrusion. Symbols as in Figure 2. FeO_T, TiO_2, P and S contents are from Zhong et al. (2002).*

8

As discussed above, the sources of parental magmas provide a key constraint on the magmatic processes. The incompatible trace element distribution patterns in the Cycle *I* (Fig. 3a) are similar to that of the asthenosphere (Arndt and Christensen, 1992) or mantle plume that gave rise to the Emeishan basalts and layered intrusions (Chung and Jahn, 1995; Xu et al., 2001). However, the simple plume-derived magma cannot account for the absent or positive Nb-Ta anomalies and markedly negative Sr anomalies. The enrichments of Nb-Ta may be attributed to contamination of the continental lithosphere mantle (CLM) composition suggested by McDonough (1990), whereas the Sr depletions may be caused by contamination of the upper crust composition estimated by Taylor and McLennan (1985). Sample (LOZ6), highly contaminated by the upper crust at the base of the intrusion, is characterized by a pronounced Sr depletion, which is consistent with the most enriched Nd-isotopic signature ($\varepsilon_{Nd}(i) \sim -2.7$). Magma parental to the remaining samples is characterized by low contents of Rb and Ba and zero to marked Sr depletion in the Cycle *I* may be slightly contaminated by the upper crust, as the involvement of a large amount of the upper crust would cause the enrichments of Rb and Ba and a significantly negative Sr anomaly. Similarly, the parental magma of Cycle *II* may also have experienced marked contamination of CLM and slight contamination of the upper crust. The Sr anomalies in Cycle *III*, except that for the sample (MCZ6) contaminated by a syenite dyke, are mainly controlled by the crystallization of plagioclase. It is possible that the magma parental to the Cycle *III* is predominantly contaminated by CLM.

Most of the samples from the three basal cycles in the Hongge intrusion exhibit similar incompatible trace element distribution patterns. This may imply that their parental magmas were derived from a plume that was subjected to different degrees of contamination of CLM and the upper crust during ascent and emplacement and thereafter experienced different processes of fractional crystallization. The suggestion is supported by the nearly homogeneous Sr-Nd isotopic signature ($\varepsilon_{Nd}(i) = -1.03 \sim +1.02$, $(^{87}Sr/^{86}Sr)_i = 0.7058\sim0.7064$). An exception, however, is the lowermost sample (LOZ6) in the intrusion (Table 2, Fig.5), which is highlighted by the Sr isotopic study of Yuan et al. (1985) [$(^{87}Sr/^{86}Sr)_i = 0.7053\sim0.7060$, calculated to 260 Ma] and Cong (1988) [$(^{87}Sr/^{86}Sr)_i = 0.7058\sim0.7067$, calculated to 260 Ma] and the Nd isotopic study of Zhang et al. (1999) [$\varepsilon_{Nd}(i) = +0.02 \sim +0.69$, calculated to 260 Ma] for the Hongge intrusion. Previous investigations have correlated the emplacement of the Hongge intrusion with the eruption of the Emeishan basalts (Liu et al., 1985; Lu et al., 1988; Zhang et al., 1999), largely on the basis of their physical and
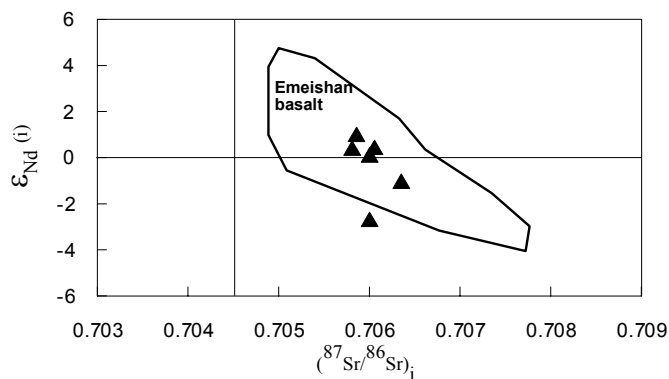

Figure 5: *Plot of initial $\varepsilon_{Nd}(i)$ and $(^{87}Sr/^{86}Sr)_i$ (t=260 Ma) for the Hongge intrusion. The field of the Emeishan basalts is after Xu et al. (2001).*

temporal proximity. This notion is further supported by the similarity in Nd-Sr isotopic distributions of the Hongge intrusion to those of the Emeishan basalts (Fig. 5). The Emeishan basalts are interpreted as having resulted from a mantle plume starting at the base of the Yangtze Craton (Chung and Jahn, 1995; Xu et al., 2001), with isotopic characteristics of $\varepsilon_{Nd}(i) \sim +5$ and $(^{87}Sr/^{86}Sr)_i \sim 0.704$ (Xu et al., 2001). The magmas parental to the Hongge intrusion may have originated from such a plume-derived magma, subjected to contamination of CLM and slight contamination of the upper crust, although quantitative constraints on contamination cannot be modelled without meaningful data on CLM and the proximal crustal rocks in the Pan-Xi area.

A remarkable decoupling of major and trace elements and Sr-Nd isotopic compositions is observed in the Hongge intrusion, as shown by the abrupt change of major and trace elements across the transition zone of individual cyclic units and the Sr-Nd (especially the immobile Nd) isotopic homogeneity. This relationship is similar to the compositional and isotopic changes in the Upper Zone of the Bushveld Complex, in which the entire Upper Zone crystallized from a magma that was thoroughly mixed before crystallization. Furthermore, the layering and mineralogical diversity of the Upper Zone was produced by internal processes (Kruger et al., 1987). It therefore appears that the Hongge intrusion may have experienced similar magmatic processes, which is in accord with the present proposal advocating new magma input, with fractional crystallization the major controlling factor in each cyclic unit.

Magma mixing and PGE mineralization

The mixing of magmas with different compositions has been invoked to explain sulphide-enriched layers (Campbell et al., 1983; Irvine et al., 1983), as well as chromite and magnetite layers (Irvine and Sharpe, 1986; Harney and Merkle, 1990; Harney and von Gruenewaldt, 1995). As discussed previously and also noted by Zhong et al. (2002), each cyclic unit in the Hongge intrusion represents a new batch of magma, which was derived from the same mantle plume, but was subjected to different degrees of contamination by CLM and the upper crust. In the present study, magma mixing between a primary and an evolved magma would occur at the bottom of Cycles *II* and *III* in the intrusion, while it is likely that Cycle *I* mainly resulted from contamination by CLM and the upper crust (including the wall rocks).

Assimilation of wall rocks resulted in chemical and isotopic similarities to those produced by addition of magma of different compositions (DePaolo, 1985). The magma parental to Cycle *I* that assimilated the Mesoproterozoic granitic gneisses and the Sinian dolomitic limestone (PXGT, 1987; Zhang et al., 1999), would cause S, Cr, Ti and Fe saturation in the contaminated magma, leading to crystallization of sulphides, titanochromite and titaniferous chromite-magnetite. The sulphides and titanochromite would facilitate the concentration of PGE, and subsequently the dense sulphides would settle downward through the unconsolidated crystal pile and become concentrated at the base of Cycle *I* (Fig. 2), as demonstrated by the previous field investigations and geochemical studies (PXGT, 1987; Liang et al., 1998; Zhong et al., 2002). However, the relatively low proportion of assimilation of wall rocks would not produce a single magnetite layer in Cycle *I* as shown in the previous studies (PXGT, 1987; Yao et al., 1993; Zhong et al., 2002).

By contrast, a new pulse of magma that is relatively enriched in PGE, Ni, Cr and MgO and depleted in incompatible trace elements, may have risen some way upwards into the evolved magma as a fountain (Campbell and Turner, 1989) in Cycle *II*. The new liquid would mix with the resident magma and cause the crystallization of an iron-titanium-chrome oxide,

which could considerably reduce the sulphur capacity of the melt (Haughton et al., 1974; Fleet et al., 1991). As a result, sulphides droplets would form and settle together with the magnetite crystals. The early-formed sulphides would be PGE-rich, but because of the strong partitioning of these PGEs into sulfides, the magma would rapidly become depleted in PGE (Naldrett et al., 1990). The sulphides would settle downward through the unconsolidated magnetite layer and concentrate in the underlying cumulates (Fig. 2). If double diffusive convection played a significant part in the generation of Cycle *II* (Lu et al., 1988), the magma that was thoroughly mixed prior to crystallization would produce the layering and multiple magnetite layers in this cyclic unit.

Such a magma mixing model might also be applicable for sulphide saturation and formation of the magnetite layers in Cycle *III*, as a new magma input has been demonstrated in this cycle. The absence of the PGE-enriched layer in Cycle *III* (which is similar to the example of the Bastard Reef in Bushveld Complex; Kruger, 1992), may be caused by the resident magma that would have been significantly depleted in PGE by the precipitation of the PGE-enriched layer in Cycle *II*, a proposal supported by recent research of Zhong et al. (2002).

CONCLUSIONS

1. Variations of major and trace elements in each cyclic unit of the Hongge intrusion are controlled by fractional crystallization, while the abrupt change of major and trace elements across the transition boundary of individual cyclic units represents the addition of a new magma.
2. These new magmas were derived from a starting mantle plume with $\varepsilon_{Nd}(i) \sim +5$ and $(^{87}Sr/^{86}Sr)_i \sim 0.704$ in origin, which was then subjected to different degrees of contamination by continental lithosphere mantle and the upper crust on the basis of trace element distributions and Sr-Nd isotopic signature.
3. The remarkable decoupling of Sr-Nd isotopic homogeneity and cyclic variations of major and trace elements implies that each cyclic unit crystallized from a magma that was thoroughly mixed before crystallization.
4. A plume-derived magma that experienced contamination of continental lithosphere mantle and assimilation of wall rocks could account for the PGE mineralization in Cycle *I*, but could not produce a single magnetite layer.
5. In Cycle *II*, a more primitive magma was injected as a fountain and blended with a more evolved magma resting on the crystal pile. Magma mixing would be responsible not only for the formation of the PGE-enriched layer, but also for the development of the magnetite layers. A similar magmatic process was repeated in Cycle *III*, although the PGE-enriched layer could not be produced due to the highly PGE-depleted evolved magma.

ACKNOWLEDGMENTS

REFERENCES

Arndt, N. T., Christensen, U., 1992, The role of lithosphere mantle in continental flood volcanism: Thermal and geochemical constraints: J. Geophys. Res., v. 97, p. 967-981.

Campbell, I. H., Naldrett, A. J., and Barnes, S. J., 1983, A model for the origin of the platinum-rich sulfide horizons in the Bushveld and Stillwater complexes: J. Petrol., v. 24, p. 133-165.

Campbell, I. H., and Turner, J. S., 1989, Fountains in magma chambers: J. Petrol., v. 30, p. 885-923.

Cawthorn, R. G., 1983, Magma addition and possible decoupling of major- and trace-element behaviour in the Bushveld Complex, South Africa: Chem. Geol., v. 39, p. 335-345.

Cawthorn, R. G., and McCarthy, T. S., 1985, Incompatible trace element behavior in the Bushveld complex: Econ. Geol., v. 80, p. 1016-1026.

Chung, S. L., and Jahn, B. M., 1995, Plume-lithosphere interaction in generation of the Emeishan flood basalts at the Permian-Triassic boundary: Geology, v. 23, p. 889-892.

Cong, B. L., 1988, Formation and evolution of the Pan-Xi paleorift: Beijing, Science Press, p.1-424 (in Chinese).

Cruft, E. F., 1966, Minor elements in igneous and metamorphic apatite: Geochim Cosmochim Acta, v. 30, p. 375-398.

DePaolo, D. J., 1985, Isotopic studies of processes in mafic magma chambers I. the Kiglapait intrusion, Labrador: J. Petrol, v. 26, p. 925-951.

Fleet, M. E., Stone, W. E., and Crocket, J. H., 1991, Partitioning of palladium, iridium and platinum between sulfide liquid and basaltic melt: Effects of melt composition, concentration and oxygen fugacity: Geochim. Cosmochim. Acta, v. 55, p. 2545-2554.

Harney, D. M. W., and Merkle, R. K. W., 1990, Pt-Pd minerals from the upper zone of the eastern Bushveld Complex, South Africa: Can. Mineral., v. 28, p. 619-628.

Harney, D. M. W., and von Gruenewaldt, G., 1995, Ore-forming processes in the upper part of the Bushveld Complex, South Africa: J. Afr. Earth Sci., v. 20, p. 77-89.

Haughton, D. R., Roeder, P. L., and Skinner, B. J., 1974, Solubility of sulfur in mafic magmas: Econ. Geol., v. 69, p. 451-467.

Hu, S. F., 2001, Petrologic geochemistry of the Hongge and Xinjie layered intrusion in the Pan-Xi area: PhD Thesis, Institute of Geology and Geophysics, Chinese Academy of Sciences, Beijing, p. 1-73 (in Chinese with English abstract).

Irvine, T. N., Keith, D. W., and Todd, S. G., 1983, The J-M platinum-palladium reef of the Stillwater Complex, Montana: II. Origin by double-diffusive convective magma mixing and implications for the Bushveld Complex: Econ. Geol., v. 78, p. 1287-1334.

Irvine, T. N., and Sharpe, M. R., 1986, Magma mixing and the origin of stratiform oxide ore zones in the Bushveld and Stillwater Complexes: In: Gallagher, M. J., Ixer, R. A., Neary, C. R., Prichard, H. M. (Eds.), Metallogeny of basic and ultrabasic rocks. Institute of Mining and Metallurgy, p. 183-198.

Kruger, F. J., 1992, The origin of the Merensky cyclic unit: Sr-isotopic and mineralogical evidence for an alterative orthomagmatic model: Aus. J. Earth Sci., v. 39, p. 255-261.

Kruger, F. J., Cawthorn, R. G., and Walsh, K. L., 1987, Strontinum isotopic evidence against magma addition in the Upper Zone of the Bushveld Complex: Earth Planet. Sci. Lett., v. 84, p. 51-58.

Liang, Y. B., Liu, T. Y., Song, G. R., and Jin, Z. M., 1998, Platinum group element deposits in China: Beijing, Metallurgical Industry Press, p. 1-185 (in Chinese).

Liu, D., Shen, F. K. and Zhang, G. Z., 1985, Layered intrusions of the Panxi area, Sichuan province: In: Zhang Y. X. (ed.) Corpus of the Panxi paleorift studies in China. Beijing, Geological Press, p. 85-118 (in Chinese).

Lu, J. R., 1996, Dynamical characteristics of the Emei mantle plume: Acta Geoscientia Sinica, v. 17, p. 424-438 (in Chinese with English abstract).

Lu, J. R., Zhang, G. D., Zhang, C. X., Gu, G. X., Liu, Y. S., and Huang, Y. N., 1988, A genetic model for layered intrusions and vanadic titanomanetite deposits in Panzhihua-Xichang area: Mineral Deposits, v. 7, p. 3-11 (in Chinese).

Luo, Y. N., 1981, The characteristics of Ti-chromite mineralization in Xinjie layered ultramafic-mafic intrusion in Panzhihua area, China: Geochimica, v. 10, p. 66-73 (in Chinese).

McDonough, W. F., 1990, Constraints on the composition of the continental lithosphere mantle: Earth Planet. Sci. Lett., v. 101, p. 1-18.

Naldrett, A. J., Brügmann, G. E., and Wilson, A. H., 1990, Models for the concentration of PGE in layered intrusions: Can. Mineral., v. 28, p. 389-408.

PXGT (Pan-Xi Geological Team of the Bureau of Geology and Mineral Resources), 1981, Geological survey report on the Xinjie V-Ti-magnetite ore district in the Miyi county, Sichuan Province: p. 15-35 (in Chinese, unpublished).

PXGT, 1987, Metallogenetic conditions and geologic characters of the Hongge vanadic titanomagnetite deposit, Sichuan: Beijing, Geological Press, p. 1- 220 (in Chinese).

SBGMR (Sichuan Bureau of Geology and Mineral Resources), 1991, Regional geology of Sichuan province: Beijing, Geological Publishing House, p. 1- 680 (in Chinese).

Sun, S. - S., and McDonough, W. F., 1989, Chemical and isotopic systematics of oceanic basalts: implications for mantle composition and processes: In: Saunders, A. D., Norry, M. J. (Eds.), Magmatism in the ocean basins. Spec. Publ. 42, Geol. Soc., Oxford, p. 313-345.

Taylor, S. R., and McLennan, S. M., 1985, The continental crust: its composition and evolution. Blackwell Scientific Publications, London, p. 1-312.

Walker, K. R., 1969, The Palisades sill, New Jersey: A reinvestigation: Geol. Soc. America Spec. Paper 3, p. 1-178.

Wilson, A. H., Lee, C. A. and Brown, R. T., 1999, Geochemistry of the Merensky reef, Rustenburg Section, Bushveld Complex: controls on the silicate framework and distribution of trace elements: Mineral Deposita, v. 34, p. 657-672.

Yang, J. H., and Zhou, X. H., 2001, Rb-Sr, Sm-Nd, and Pb isotope systematics of pyrite: Implications for the age and genesis of lode gold deposits: Geology, v. 29, p. 711-714.

Yao, P. H., Wang, K. N., Du, C. L., Lin, Z. T., and Song, X., 1993, Records of China's iron ore deposits: Beijing, Metallurgic Industry Press, p. 638-641 (in Chinese).

Xu, Y. G., Chung, S. L., Jahn, B. M., and Wu, G. Y., 2001, Petrologic and geochemical constraints on the petrogenesis of Permian-Triassic Emeishan flood basalts in southwestern China: Lithos, v. 58, p. 145-168.

Zhang, C. J., Wang, Y. L., Li, X. L., Xiu, S. Z., and Huang, Y. J., 1998, Geochemistry of platinum-group-elements in mafic-ultramafic rocks from the Xinjie intrusion: Geochimica, v. 27, p. 458-466 (in Chinese with English abstract).

Zhang, Z. Q., Lu, J. R., and Tang, S. H., 1999, Sm-Nd ages of the Panxi layered basic-ultrabasic intrusions in Sichuan: Acta Geologica Sinica, v. 73, p. 263-271 (in Chinese).

Zhong, H., Zhou, X. H., Zhou, M. F., Sun, M., and Liu, B. G., 2002, Platinum-group element geochemistry of the Hongge Fe-V-Ti deposit in the Pan-Xi area, southwestern China: Mineral Deposita, v. 37, p. 226-239.

Zhou, M. F., Malpas, J., Song, X. Y., Robinson, P. T., Sun, M., Kennedy, A. K., Lesher, C. M., and Keays, R. R., 2002, A temporal link between the Emeishan large igneous

province (SW China) and the end-Guadalupian mass extinction: Earth Planet. Sci. Lett., v. 196, p. 113-122.

Zhou, M. F., Kennedy, A. K., Sun, M., Malpas, J., and Lesher, C. M., Neo-Proterozoic arc-related mafic intrusions in the northern margin of South China: Implications for accretion of Rodinia: J. Geol. (in press).

_____oOo_____